AIP | Applied Physics Letters

# Correlating reduced fill factor in polymer solar cells to contact effects

Dhritiman Gupta, Monojit Bag, and K. S. Narayan

Citation: Applied Physics Letters **92**, 093301 (2008); doi: 10.1063/1.2841062
View online: http://dx.doi.org/10.1063/1.2841062
View Table of Contents: http://scitation.aip.org/content/aip/journal/apl/92/9?ver=pdfcov
Published by the AIP Publishing



# Correlating reduced fill factor in polymer solar cells to contact effects

Dhritiman Gupta, Monojit Bag, and K. S. Narayan[a)]
*Jawaharlal Nehru Centre for Advanced Scientific Research, Jakkur P.O., Bangalore 560064, India*

(Received 16 October 2007; accepted 16 January 2008; published online 3 March 2008)

A probable limiting factor for efficiency and fill factors of organic solar cells originates from the cathode-polymer interface. We utilize various forms of cathode layer such as Al, Ca, oxidized Ca, and low melting point alloys in model systems to emphasize this aspect in our studies. The current-voltage ($JV$) response in the fourth quadrant indicates a general trend of convex shaped $JV$ characteristics ($d^2J/dV^2>0$) for illuminated devices with good cathode-polymer interfaces and linear or concave $JV$ responses ($d^2J/dV^2<0$) for inefficient cathode-polymer interfaces. © *2008 American Institute of Physics*. [DOI: 10.1063/1.2841062]

Organic solar cells have emerged as a potential option to meet the growing need of renewable energy source. The power conversion efficiency (PCE) of bulk heterojunction (BHJ) polymer solar cells (PSCs) based on solution processible blend of poly(3-hexylthiophene) (P3HT) and [6,6]-phenyl-$C_{61}$-butyric acid methyl ester (PCBM) has reached up to 5% (Refs. 1 and 2) including recent report of PCE $\approx$6% in solution-processed PSC in a tandem cell geometry.[3] In BHJ solar cells, active layer bulk-morphology plays an important role in transport processes and is controlled by the factors such as solvent properties, drying and annealing conditions,[2] and appropriate distribution of the two components.[4] A crucial factor to realize the maximum impact of the different strategies finally depends on better fill factor (FF) of the devices which is more sensitive to the polymer-metal interface morphology unlike other parameters such as the open circuit voltage ($V_{OC}$) and short circuit current density ($J_{SC}$). Realistic deposition conditions of the cathode lead to a variety of interfacial features, of which some are current limiting and detrimental. We emphasize this aspect in our studies using a set of high performance model organic donor-acceptor (DA) blend systems, by monitoring the dependence of the solar cell parameters.

In case of perfect Ohmic contacts (noninjecting in reverse bias mode), the behavior of the illuminated $JV$ response depends on the drift length ($L_D$) ratio ($b$) of the electrons ($e$) and holes ($h$) which is given by the ratio of their mobility ($\mu$)—lifetime ($\tau$) product ($b=\mu_e\tau_e/\mu_h\tau_h$).[5] For balanced transport ($b\sim1$), photocurrent ($J_{ph}$) varies linearly with $V$ at low voltage regime and then saturates at higher voltage. However, in case of unbalanced $\mu\tau$-limited transport ($b<1$ or $b>1$) carrier accumulation takes place near both the contacts modifying the field and in absence of any recombination, the thickness ($l$) of the accumulation region is governed by the smaller $\mu\tau$ product. In an extreme case ($b\gg1$ or $b\ll1$), the field in the region of slow carrier accumulation becomes almost equal to the applied external voltage and the resulting current becomes space-charge limited (SCL). In the SCL and $\mu\tau$-limited cases, the $J_{ph}$ shows a square root dependence on $V$, however, the intensity ($P$) dependence of $J_{ph}(P)$ varies as $P^{3/4}$ in case of SCL and linearly in $\mu\tau$ limited case. SCL behavior has been demonstrated for a blend of PPV derivative and PCBM where $\mu_h$ in PPV phase ($\mu_h\sim3.2\times10^{-5}$ cm$^2$/V s) is two orders of magnitude lesser than the $\mu_e$ in the PCBM phase ($\mu_e\sim4\times10^{-3}$ cm$^2$/V s).[6] Apart from the mobility mismatch, thickness ($L$) of the active polymer layer also plays a role. A transition from non-SCL to SCL has been observed in the PPV-PCBM blend system by increasing $L$.[7] SCL-$J_{ph}$ limits the FF of the device, maximum possible FF being 42%.[6] For balanced transport, a DA pair with comparable $\mu\tau$ is always preferable. From this point of view, DA pairs, P3HT ($\mu_h\sim10^{-4}$ cm$^2$/V s)-PCBM ($\mu_e\sim10^{-3}$ cm$^2$/V s), and poly[2-methoxy-5-(2-ethylhexyloxy)-1,4-phenylene vinylene] (MEHPPV)-CyanoPPV (CNPPV) ($\mu_h=\mu_e\sim10^{-5}$ cm$^2$/V s) should show comparable efficiency. Experimentally, in spite of a higher $V_{OC}$ of $\sim$1.2 V, all active-polymer solar cells based on MEHPPV-CNPPV blend has much lower FF ($\approx$30%) (Refs. 8–12) resulting in a lower PCE as compared to P3HT-PCBM (FF$\approx$68%) (Ref. 2) and has been attributed to the low $\mu$ in PPV systems and consequent low exciton dissociation rate.[12] Solar cells based on small molecules are also capable of giving high FF (>50%).[13] However, lowering of FF (<25%) due to the "S-shaped" $JV$ response has been observed in these systems as well.[14,15] The characteristic S-shaped $JV$ curve is the signature of a counterinjecting diode which arises due to charge accumulation near one of the electrode. Charge carrier accumulation can be a contact-driven process and we demonstrate the importance of contact effects to the FF in the two model systems of P3HT-PCBM and MEHPPV-CNPPV where transport is balanced.

P3HT-PCBM blend based PSC was prepared using standard protocol[1–4] on indium tin oxide substrates coated with a layer of poly(ethylenedioxythiophene):poly(styrene sulfonic acid). P3HT and PCBM in chlorobenzene of concentration 25 mg/mL were mixed (in 1:1 weight ratio), stirred, filtered, and subsequently, spin coated to get uniform films of thickness less than 100 nm. Al and Ca (followed by a 200 nm thick Al deposition) depositions were done through shadow mask in a base pressure of $10^{-6}$ mbar. The typical device area was 10 mm$^2$. The fabrication details of MEHPPV-CNPPV devices have been provided elsewhere.[8]

The $JV$ characteristics measured in the dark ($J_D$) and under illumination ($J_L$) with white light are shown in Fig. 1 for P3HT-PCBM solar cell with Ca cathode. $J_L(V)$ gives rise to a FF of 53% under low-white light illumination leading to a moderate PCE $\approx$2.1% (neglecting reflection losses). Simi-

[a)]Electronic mail: narayan@jncasr.ac.in.



 

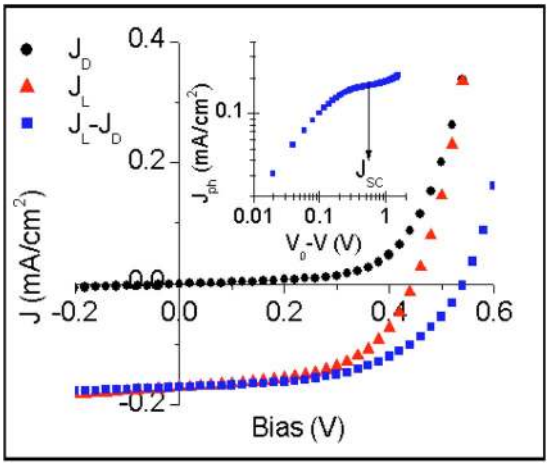


FIG. 1. (Color online) *JV* characteristics of a P3HT:PCBM solar cell with active area of 4 $mm^2$. The device shows $J_{SC}$=0.18 $mA/cm^2$, $V_{OC}$=0.44 V, compensation voltage $V_0$=0.54 V, and FF=53% under white light illumination with power density of 2 $mW/cm^2$. Inset depicts $J_{ph}$ vs $(V_0-V)$.

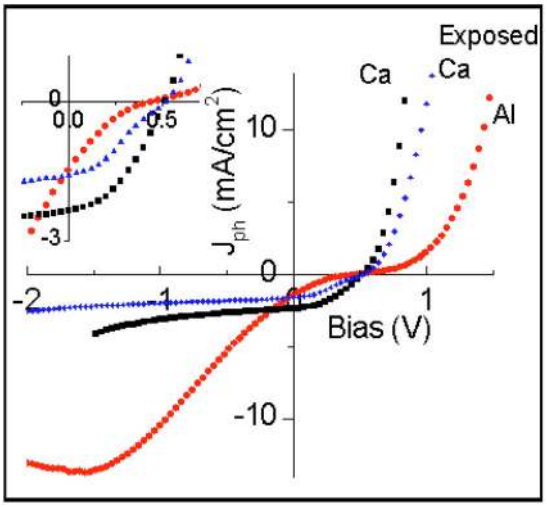


FIG. 2. (Color online) *JV* characteristics of a P3HT-PCBM solar cell with Al (●), Ca/Al (■), and exposed Ca (▲) cathodes. Under white light illumination of 20 $mW/cm^2$, Al device shows FF of 12.5%. $J_{SC}$=1.47 $mA/cm^2$ and $V_{OC}$=0.46 V. In calcium device, FF=37.8%, $V_{OC}$=0.52, $J_{SC}$=2.35 $mA/cm^2$. Exposed Ca gives rise to barrier which in turn reduces FF to ≈28% with $J_{SC}$=1.58 $mA/cm^2$ and $V_{OC}$=0.54 V.

lar efficiency was achieved under AM1.5 (100 $mW/cm^2$) illumination (supplementary Fig. 1 in Ref 16). The photocurrent ($J_{ph}$=$J_L$-$J_D$) against the effective applied bias voltage ($V_0-V$) is depicted in the inset of Fig. 1, where $V_0$ is the compensation voltage, defined by the voltage at which the $J_{ph}$=0. $J_{ph}$ linearly increases with voltage at low effective field ($V_0-V\leqslant 0.1$) and for high effective field ($V_0-V>0.1$), $J_{ph}$ gradually saturates to the value, $qG(E,T)L$ and becomes independent of $V$ (assuming no charge carrier recombination),[17] where $q$ is the electronic charge and $G(E,T)$ is the generation rate of free carriers ($T$ is the temperature). These devices (with $L<100$ nm) have no significant SCL contribution. The dissociation efficiency is quite high and weakly dependent on field since one-sixth of the total photogenerated charge carriers [which give rise to saturation photocurrent in high effective field region ($V_0-V>0.1$)], is already dissociated in the low effective field regime ($V_0-V\approx 0.01$) (Fig. 1, inset). The performance of PSC can be adjudged by the second derivative ($d^2J/dV^2$) or the extent of convexity which is >0 in the region $V_{knee}<V<V_{OC}$, where $V_{knee}$(≈0.18 V) is the knee voltage.

Replacing the Ca electrode with Al gives rise to a point of inflection near $V_{OC}$ and subsequent concavity in the fourth quadrant ($d^2J/dV^2<0$ in the range $V_{knee}<V<V_{OC}$) of the *JV* characteristics with similar magnitude of $J_{SC}$ and $V_{OC}$ (Fig. 2). Work function differences do not significantly alter $V_{OC}$ which is in accordance with the idea that $V_{OC}$ is controlled primarily by the energy levels of the DA materials. The morphology and the chemical integrity of the interface play crucial roles in the $J(V)$ mechanism. Slow evaporation rate or an inverted geometry has been speculated to be useful to get a better PCE with Al cathode.[18,19] In our case, Al electrode formed by slower deposition rate appeared to improve the FF (supplementary Fig. 3 in Ref. 16) with magnitude approaching the values corresponding to Ca electrode (which was less sensitive to the deposition rate) devices. Extremely fast deposition rate gave rise to the concavity in the *JV* characteristics. The inhomogenity of interfaces is higher with a rapid evaporation rate of metal and is evident in the surface images (supplementary Figs. 4 and 5 in Ref. 16). The origin of different FF depending on the deposition conditions can be attributed to a variety of physical and physiochemical factors. A simplistic analysis of bias dependent schottky-type depletion width can explain the lowering of the $J_{ph}$ in $0<V<V_{OC}$ region. In maximum power point, the device is operating under a bias of 220 mV (corresponding field $\approx 2.2\times 10^4$ V $cm^{-1}$) which makes the current at this point ($J_{max}$) to be only 7% of $J_{SC}$. This argument is not applicable for PSCs with a slower, more uniform coated Al layer. The difference can be reconciled to the metal-polymer reaction leading to different barrier levels and widths under different thermodynamic conditions.[20] The reduction of FF can also arise due to the chemical degradation of the metal-polymer interface. These observations were confirmed on two weeks exposure of the samples with Ca cathode which showed the signature of degradation due to exposure to ambient where the appearance of a "kink" (second point of inflection where $d^2J/dV^2$ changes its sign from negative to positive) in the fourth quadrant reduces the FF by half (Fig. 2). The kink in the fourth quadrant, which is suppressed at low light intensity (<10 $mW/cm^2$) (supplementary Fig. 2 in Ref. 16), is indicative of a defect induced recombination process. A nonuniform contact or incomplete coverage of the metal over the polymer surface can result in a scenario of charge accumulation leading to a barrier formation which can possibly explain the resulting $J(V)$ response.

The situation is, however, different in case of PSCs based on MEHPPV-CNPPV blends. In Fig. 3, the *JV* characteristics of a MEHPPV-CNPPV device indicate FF ≈20% for Al and 28% for Ca electrodes. $J_{SC}$ is one order of magnitude smaller in Al devices due to the higher series resistance ($R_SA\sim 95$ kΩ $cm^2$) as compared to Ca devices ($R_SA\sim 0.4$ kΩ $cm^2$). The dark-*JV* characteristics is almost symmetric in the entire voltage range (−2−+2 V). The high $J_D$ in the reverse bias region can be attributed to the carrier injection through the CNPPV phase in reverse bias mode and not to the mechanical pinholes. Occurrence of high reverse $J_D$ has been observed in devices with different area (ranging from 1 to 25 $mm^2$). The strong increase in $J_D$ in the forward bias above 0.8 V is an indication of current through MEHPPV phase. This suggests that MEHPPV phase also connects

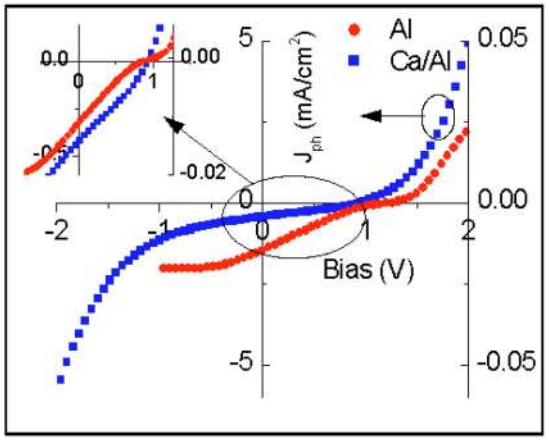


FIG. 3. (Color online) The *JV* characteristics of a MEHPPV-CNPPV device with Al (●) and Ca/Al (■) cathodes, under monochromatic light illumination of power density of 1 mW/cm$^2$. For Al cathode, $J_{SC}$=0.015 mA/cm$^2$, $V_{OC}$=1.18 V, and FF=20%. For Ca device, $J_{SC}$=0.43 mA/cm$^2$, $V_{OC}$=0.76 V, and FF=28%.

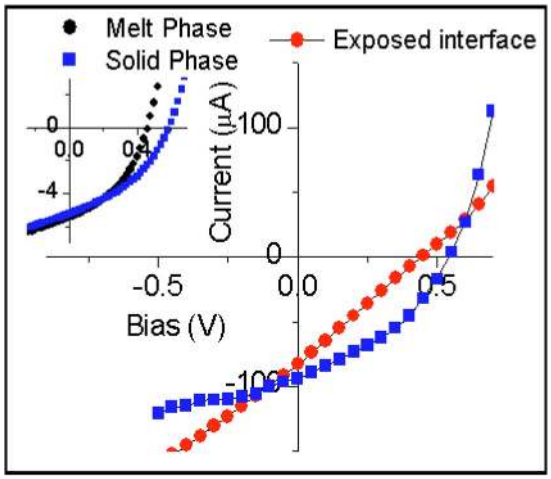


FIG. 4. (Color online) *IV* characteristics of a P3HT-PCBM blend solar cell (active device area was ~4 mm$^2$) with meltable alloy as the cathode showing the FF≈37.66% and 24.8% when the interface is contaminated. FF in the melt phase is 41% and 38% in the solid phase.

to both the electrodes and the blend is cocontinuous. The reason for poor fill factor can be attributed to the poor rectification property from the high reverse injection current which competes with the diffusion current under illumination apart from the lower exciton dissociation rate arising from the low carrier mobility in these systems.[12]

We further confirm our hypothesis based on our study with a low melting point (MP) cathode alloy of In–Sn–Pb–Bi (~58 °C). This alloy forms an Ohmic contact with the polymer and is a good electron collecting cathode. This thermally deformable cathode layer also provides a direct evidence of the importance of the cathode morphology on the FF. P3HT-PCBM solar cell characteristics with this cathode were carried out on a hot stage in a microscope platform. This system using the low MP alloy can be used to gauge the effects caused by physical and the physiochemical features at the interface. The physical effect appear in terms of the effective contact area between the metal alloy and the semiconductor while the trapped oxygen and moisture upon freezing the sample acts as the source for an additional oxide-barrier layer. The similarity of the *IV* in the melt phase (at 60 °C) and solid phase (at 45 °C) of the cathode in the device shown in Fig. 4 indicates similar contact area for the two phases with a high FF of >40%. However, during the solidification process, if defects are introduced, the *IV* drastically changes with a significant field dependent reverse bias $I(V)$, as shown in Fig. 4, and a low FF of <24%. The effects related to the heating and cooling rates of the cathode and the consequent structures at the interface are currently being pursued in our laboratory.

In conclusion, we have observed that the shape of the *JV* characteristics in the power generating fourth quadrant strongly depends on the quality of polymer cathode interface and does not always bear the fingerprint of bulk material properties. A partial metal coverage or a chemically modified layer can reduce the fill factor drastically in an otherwise efficient solar cell device. The most commonly known bulk-limiting factors, such as space charge effect due to difference in mobility numbers and strong field dependence of dissociation efficiency, seem to be secondary in these cases. These results show a clear distinction between generation-transport occurring in the bulk and carrier collection efficiencies which is determined by cathode-polymer interface morphology. An identifiable direct signature of this effect manifests in the form of the profile of the *JV* characteristics.

We thank Professor S. Ramakrishnan for providing us with MEHPPV and helping us in synthesizing CNPPV.

[1]K. Kim, J. Liu, M. A. G. Namboothiry, and D. L. Carroll, Appl. Phys. Lett. **90**, 163511 (2007).
[2]G. Li, V. Shrotriya, J. Huang, Y. Yao, T. Moriatry, K. Emery, and Y. Yang, Nat. Mater. **4**, 864 (2005).
[3]J. Y. Kim, K. Lee, N. E. Coates, D. Moses, T.-Q. Nguyen, M. Dante, and A. J. Heeger, Science **13**, 222 (2007).
[4]M. Reyes-Reyes, K. Kim, and D. L. Carroll, Appl. Phys. Lett. **87**, 083506 (2005).
[5]A. M. Goodman and A. Rose, J. Appl. Phys. **42**, 2823 (1971).
[6]V. D. Mihailetchi, L. J. A. Koster, and P. W. M. Blom, Phys. Rev. Lett. **94**, 126602 (2005).
[7]M. Lenes, L. J. A. Koster, V. D. Mihailetchi, and P. W. M. Blom, Appl. Phys. Lett. **88**, 243502 (2006).
[8]D. Gupta, D. Kabra, K. Nagesh, S. Ramakrishnan, and K. S. Narayan, Adv. Funct. Mater. **17**, 226 (2007).
[9]A. J. Breeze, Z. Schlesinger, S. A. Carter, H.-H. Hörhold, and H. Tillmann, Sol. Energy Mater. Sol. Cells **83**, 263 (2004).
[10]T. Kietzke, D. Neher, and H.-H. Hörhold, Chem. Mater. **17**, 6532 (2005).
[11]M. Granström, K. Petritsch, A. C. Arias, A. Lux, M. R. Andersson, and R. H. Friend, Nature (London) **395**, 257 (1998).
[12]M. M. Mandoc, W. Veurman, L. J. A. Koster, B. de Boer, and P. W. M. Blom, Adv. Funct. Mater. **17**, 2167 (2007).
[13]S. B. Rim, R. F. Fink, J. C. Schöneboom, P. Erk, and P. Peumans, Appl. Phys. Lett. **91**, 173504 (2007).
[14]Q. L. Song, M. L. Wang, E. G. Obbard, X. Y. Sun, X. M. Ding, X. Y. Hou, and C. M. Li, Appl. Phys. Lett. **89**, 251118 (2006).
[15]V. P. Singh, R. S. Singh, B. Parthasarathy, A. Aguilera, J. Anthony, and M. Payne, Appl. Phys. Lett. **86**, 082106 (2005).
[16]See EPAPS Document No. E-APPLAB-92-065806 for additional experimental results. This document can be reached through a direct link in the online article's HTML reference section or via the EPAPS homepage (http://www.aip.org/pubservs/epaps.html).
[17]V. D. Mihailetchi, L. J. A. Koster, J. C. Hummelen, and P. W. M. Blom, Phys. Rev. Lett. **93**, 216601 (2004).
[18]M. Glatthaar, M. Riede, N. Keegan, K. Sylvester-Hvid, B. Zimmermann, M. Niggemann, A. Hinsch, and A. Gombert, Sol. Energy Mater. Sol. Cells **91**, 390 (2007).
[19]V. Djara and J. C. Bernède, Thin Solid Films **493**, 273 (2005).
[20]E. Ahlswede, J. Hanisch, and M. Powalla, Appl. Phys. Lett. **90**, 063513 (2007).